Diagnosis of Prostatic Intraepithelial Neoplasia in Luminal Cells Using Raman Spectroscopy

Suneetha Devpura[1], Jagdish Thakur[1], Seema Sethi[2],
Vaman M. Naik[3], Fazlul Sarkar[2], Wael Sakr[2] and Ratna Naik[1]
[1]Wayne State University, Detroit, MI
[2]Pathology, Karmanos Cancer Institute, Detroit, MI
[3]Univeristy of Michigan-Dearborn, Dearborn, MI,
USA

1. Introduction

Prostate cancer is the second most common cancer among men in worldwide based on the statistics in 2008 (Jemal, 2011). In 2008, 903,500 (14%) new cases are recorded and about 258,400 (6%) people died. The highest incidence rates are observed in the developed countries in Oceania, Europe, and North America. Since the introduction of Prostate Specific Antigen (PSA) test, which measures the level of PSA in patients' blood, for prostate cancer screening the mortality rate has decreased due to its early detection and treatment (Oesterling, 1991, Shroder, 2009). The other method for detecting the prostate cancer involves a Digital Rectal Examination (DRE) to check for growths in or enlargement of the prostate gland in men. If there is a tumor growth in the prostate, it can often be felt as a hard lump. To further confirm the tumor, a pathological examination is performed on surgically removed tissues from the suspected areas of prostate and grade of the cancer (Humphrey, 2004) is determined. According to the current policy, the age limit to obtain PSA has been lowered to 40 years. In addition, decision to perform biopsies is not followed by PSA and DRE alone, other factors such as patient age, PSA velocity, PSA density, family history, ethnicity, etc are also considered (Caroll, 2009). One of the common tissue extraction methods is needle biopsy. A recent study has shown that a Target Scan biopsy method has better accuracy over conventional practice to locate the malignant tissues (Andriole, 2007). Combined examination of PSA, DRE, and pathological tests provides a better diagnostic ability for prostate cancer (Partin, 1997). Once a patient is diagnosed with cancer, there are a few early therapeutic procedures available for patient depending on a variety of different factors, like the stage of the tumor, health of the patient and his age etc. These procedures are: radical prostatectomy, external beam radiotherapy, brachytherapy, high intensity focused ultrasound, and cryotherapy (Hricak, 2009). After radical prostatectomy, number of biopsies containing tumor and biopsy perineural invasion are found to be independent predictors of the recurrence of the disease, provided that the patients' PSA is more than 10ng/ml (Quinn, 2003). Prostate instraepethelial neoplasia (PIN) is a precursor lesion in prostate cancer which can be of high or low grade category. Usually PIN is referred to as high grade if it is capable of developing into cancer within the next 10 years (Bostwick &

Qian, 2004) or so. A study has suggested that antiactivity of certain dietary flavonoids prevents the progression of high grade PIN to cancer (Kandaswami, 2005). However, this hypothesis could not be established in a randomized double-blind study performed with 303 men in twelve Canadian centers. These men were given soy, vitamin E, and selenium on daily basis for three years. The results were not statistically significant to show their effects on decreasing the progression of cancer or eliminating it (Fleshner, 2011).

Detection and confirmation of prostate cancer is very crucial for its successful treatment and survival rate. Sometimes the standard screening programs can provide misleading results leading to wrong or over-treatments and occasionally to fatal consequences. The interpretations of histological examination of biopsies, considered as the "gold standard" for diagnosis, are often subjective and can vary significantly from one pathologist to another (Allbrook, 2001). Hence, it is imperative to detect the state of the disease with a method which is objective and capable of providing results within a very short period of time (1-2 minutes). Optical spectroscopy techniques are very well suited for these types of goals, and in addition, they are also capable of probing disease at cellular level. Raman spectroscopy is one of the optical techniques which is currently extensively investigated as a diagnostic tool for detection of different types of cancers (Laserna, 1996). This optical method can provide information about the changes in the concentrations of the constituent biomolecules of tissues and detect the progression or state of the disease. In Raman spectroscopy measurements, a laser light is incident on a sample which interacts with its molecules and gets scattered. Majority of the light scatters elastically; however a very small fraction of it scatters inelastically carrying information about the nature of the sample's molecules, their mutual interaction, and their relative concentrations in the sample (Raman, 1928). The chemical nature of molecules can be uniquely determined from a set of their vibrational energy levels and Raman spectroscopy has the capability to measure these vibrational energy levels (Gelder, 2007, Movasaghi, 2007). This powerful capability of the Raman spectroscopy provides a fundamental motivation to develop this optical technique as an objective diagnostic tool for early detection of cancers. The changes in biochemical composition of a cancerous tissue could be detected through the observed changes in Raman band intensities compared to those of normal tissue. As the biochemical compositions of a tissue or cell begin to change from its normal values, it can trigger the onset of a cancer, and Raman spectroscopy has the potential to detect those initial compositional changes. So this technique can be used to diagnose pathological condition of organs and progression of disease. Currently, the potential of this technique are being tested to detect different types of cancers: breast, prostate, bladder, cervix, skin, larynx, head and neck squamous cell carcinoma, etc. and determine their unique spectra features (Stone, 2003, Keller, 2006, Devpura, 2010, 2011). Raman spectroscopy is able to identify prostate cancer from benign with 89% accuracy in snap frozen biopsies *in vitro* (Crow, 2003). Reduction in glycogen and increment in nucleic acid contents of malignant areas are observed through Raman bands. Sensitivity of differentiating cancer grades, Gleason score 7, less than 7, and greater than 7 are more than 81%. In another study, prostate cancer was identified with 94% accuracy compared to benign and prostate intraepithelial neoplasia (Devpura, 2010). In addition, Gleason score 6, 7, and 8 were distinguished with more than 81%. However, this needs to be validated with additional studies on more tissue specimens. Bladder and prostate cancers were also investigated using a fiber optic near-infrared Raman spectrometer and an overall accuracy of 84% and 86%, respectively, was observed (Crow, 2005). An attempt to construct an integrated Raman and angular-scattering microscope was

made to collect both Stokes-shifted light and elastic light (Smith & Berger, 2009) to improve the detection performance and accuracy. This will allow characterizing simultaneously the size of cell and its chemical information. Recently, Raman spectroscopy was successfully used to determine the variation of chemical composition of a cell in response to a drug treatment. A threshold concentration of a toxic amount of *Nerium Oleander* was determined (Saha, 2009). This demonstrates that this technique can be used in drug designing application.

Due to advancement in diagnostic technologies and treatment modalities, most of the cancers can be cured if detected in their early stages. Cancer is basically a disease in which abnormal cells divide without any control and these cancerous cells are able to invade other tissues, and by this process the disease spreads to other organs. Hence, it certainly will be of great advantage to detect biomolecular compositional changes at cellular level, particularly in these proliferating cells. In this study, we have focused our study on luminal cells of PIN and compare their spectral features of benign epithelia (BE) and cancerous cells of the prostate tissues. To the best of our knowledge, this is the first report of such an investigation. It is important to compare luminal cells of each pathological category since basal cells are absent in the epithelium of microacinar structures of the prostate cancer. In addition, we have investigated the stroma surrounding BE, PIN, and cancerous micro acinar clusters.

The interaction between prostatic stroma and the epithelial cells is somewhat different from the stromal cells in prostate tumors (Bowsher & Carter, 2006). The prostatic stroma, which consists of fibromuscular matrix enclosing the prostatic ducts, limits the proliferation of the epithelia unlike the stroma in the prostatic tumors which contain fibroblasts or myofibroblasts. The stroma bordering prostatic tumors is called "reactive stroma" or "carcinoma associated fibroblasts" (Bowsher & Carter, 2006). It is imperative to explore the spectral features of the stromal cells in BE, PIN, and tumor stages and understand its linkage with cancer and its progression. It appears that the reactive stroma in prostate initiates the carcinogenesis and helps its progression (Olumi, 1999, Hayward, 2001, Niu & Zia, 2009).

2. Materials and methods

In this study, we used a Renishaw RM1000 Raman microscope-spectrometer with a 785 nm laser excitation source. RM1000 is equipped with a CCD (charged-coupled device) detector, an automated *xyz* stage (ProScan II) with WIRE 2.0 software to control the recording of the Raman spectra. 50x objective was used to collect data from the tissue specimens with laser power of about 20 mW focused to a spot size of ~ 2 µm diameter on the tissue specimens. Each Raman spectrum was averaged over three scans with 20 s integration time to obtain a good signal-to-noise ratio. The scattered light was collected in a back scattering geometry and dispersed using a 1200 lines/mm grating.

2.1 Preparation of tissues for Raman spectroscopy

Tissue specimens which are embedded in paraffin wax were obtained from Karmanos Cancer Center and Harper University Hospital in Detroit, MI, USA, and were processed at

the University Pathology Services at Karmanos Cancer Center. In this study, we specifically selected the tissue specimens which were purely BE, PIN or cancerous. For each specimen, two parallel adjacent sections were cut. One 5 μm thick section was stained with Haematoxylin and Eosin (H&E) and was used for pathological examination, and the second 10 μm thick layer was used for Raman spectroscopic measurements. The H&E stained slides were reviewed by three experienced pathologists and none of the cases studied here found to be in dispute. The paraffin wax was removed from the 10 μm thick tissue sections using xylene and ethanol baths following the procedures described in Devpura, 2010 and 2011. It is noted that the incomplete removal wax residues gives rise to strong and sharp Raman bands that interfere with the Raman bands of the tissue samples at 1063, 1130, 1296, 1436, and 1465 cm^{-1} (Ó Faoláin, 2005). In our spectra, we did not observe any of the sharp bands associated with wax. Assuming that the morphological features do not change across a few micrometer thick layers, the H&E stained layer was used as a guide to collect the Raman spectra from the specific sites of the adjacent unstained deparaffinized tissue section.

2.2 Raman spectroscopic measurements

A total of 34 tissue specimens obtained from 33 patients were used in this study. Out of these, 12 specimens were benign, 11 were PIN, and 11 were cancerous with a grade of 3. The Raman spectra were recorded from the unstained tissue section. The appropriate regions on the unstained tissue section were identified with the help of the adjacent stained section with regions marked by pathologist as BE, PIN, cancer, and stroma. The identification of these regions was done with an optical microscope to make sure the data were collected only from the marked regions. When collecting Raman spectra, the laser beam was focused only on the luminal cells (Figure 1). The regions marked with elliptical symbols in the Figure 1 show the regions from where the Raman spectra were collected. In addition, it was made sure that each Raman spectrum was taken from a different region of luminal cells. The Raman spectra were collected in the 500-1900 cm^{-1} region. The 600-1800 cm^{-1} region is commonly known as the "biological window" where most of the biomolecules show intense Raman excitations. An extra 100 cm^{-1} extended region were recorded at both ends of the Raman spectra to avoid any artifacts which may occur while removing the fluorescence background
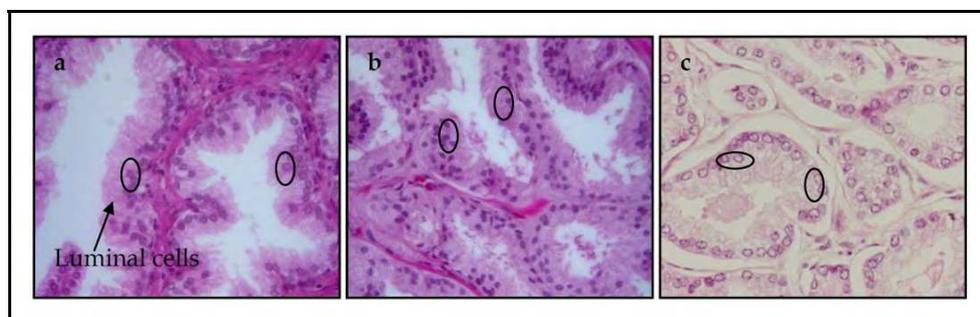

Fig. 1. Pathology pictures of (a) BE tissue, (b) PIN, and (c) Cancer (images are taken with 40x magnification). Elliptical symbols represent locations of the Raman measurements from the corresponding unstained tissue.

from each spectrum. A total of 1220 Raman spectra were collected from the tissue samples in which 207, 202, and 208 are from the luminal cells of BE, PIN, and cancer (grade 3), respectively, and the remaining (201 spectra each) from the corresponding stromal regions. The Raman measurements of stromal cells in cancer tissues were obtained from the bordering regions of the grade 3 micro acinar clusters.

2.3 Raman data processing and chemometric analysis

The collected Raman spectra were examined for non-standard noise and those with such noise were discarded from the database used for analysis. The spectra used in the analyses were cleaned from any spurious bands due to cosmic rays and noise by using wavelets method (Cao, 2007). The fluorescence background from each spectrum was removed with minmax adaptive algorithm that requires no apriori knowledge of the spectra. Finally, each spectrum was normalized with respect to the highest intensity band in the spectrum. Multivariate/chemometric statistical method, like principal component analysis, PCA, (Jolliffe, 2002) which determines correlation in the variance, was used to detect trends in the data set. The data was further analyzed using discriminant function analysis, DFA (Klecka, 1980) to classify the data. First, the data was analyzed using PCA which reduces the dimensionality of the original data set from 601 variables to 19 new variables, called the eigenvectors. These new variables captured 97% of the variance of the data. Examination of the first two eigenvectors show distinct trends in the data representing BE, PIN, and cancer. These new fewer variables carrying most of the variance of the data are useful for determining the groups in the data. To find classes in the data, we have performed DFA using 19 eigenvectors as the input variables. The classification of each pathological state is done using the leave-one-out method, where each data set is considered a new case and compared with the rest of the data pool.

3. Results and discussion

The average Raman spectral features of BE, PIN, and cancer are shown in Figure 2. We see changes in the peak intensities of most of the Raman bands (Raman band assignments are listed in the table 1) in the spectra of PIN compared to the spectra of BE and cancer tissues. These changes are fundamentally related to the changes in the concentrations of the biochemicals of BE luminal cells. Significant changes are in the region from 600 cm^{-1} to 1145 cm^{-1} which are shown in the lower panel of the Figure 2. Some of the changes are noteworthy: the band at 726 cm^{-1} (assigned to ring breathing mode of DNA/RNA bases) becomes quite intense in PIN, and in addition the Raman bands at 853 cm^{-1}, 931 cm^{-1} (v_{C-C} stretching mode of protein), 960 cm^{-1}, and 1090 cm^{-1} (symmetric phosphate stretching vibrations) also show an increase in their intensities when pathological state of cell changes from BE to PIN. While the bands at 1605 cm^{-1} and 1667 cm^{-1} (amide I) showed decrease in their intensities. When comparing the average spectral changes of PIN with cancer, we see that the peak intensities at 780 cm^{-1}, 1240 cm^{-1} (proline, tyrosine), 1330 cm^{-1} and 1605 cm^{-1} are enhanced when pathological state of luminal cells changes from PIN to cancer, while the bands at 726, 853, 931, 960, and 1090 cm^{-1} show decrease in their intensities which show similar trend like the bands of BE. The Raman bands at 780 cm^{-1} and 878 cm^{-1} showed progressive increase in their intensities when cells changes from BE to PIN and then to

cancer. These Raman bands should be further investigated for their possible association with progression of prostate cancer and perhaps their use as diagnostic variables.
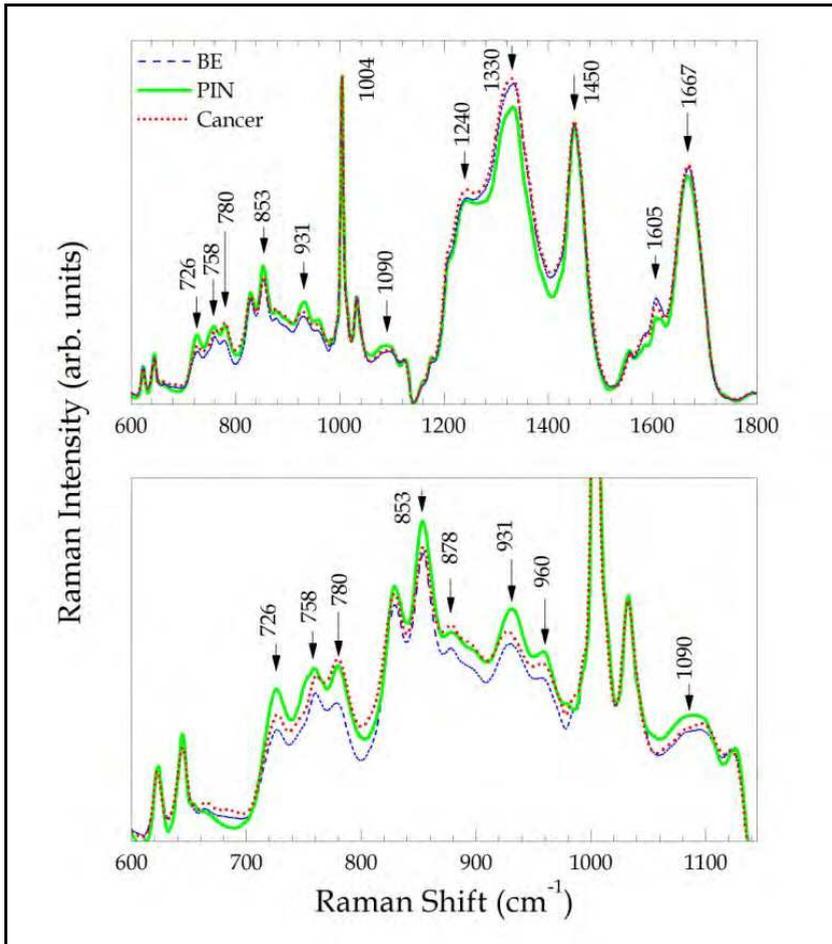

Fig. 2. Average Raman spectra of BE (blue dash line), PIN (green), and Cancer (red dotted line). The lower panel shows the Raman spectral range of 600-1145 cm^{-1}.

Raman Shift (cm^{-1})	Peak Assignment
726	A ring breathing mode of DNA/RNA bases
758	Symmetric breathing of tryptophan
780	DNA/uracil ring breathing mode
829	Tyrosine, phosphodiester, O-P-O stretching DNA/RNA
853	Ring breathing mode of tyrosine, C-C stretch of proline ring, glycogen
878	Tryptophan, hydroxyproline, C-O-C ring
931	C-C stretch, α-helix, protein band
960	Cholesterol, phosphate of HA
1004	Phenylalanine
1032	Phenylalanine, proline
1081	Typical phospholipids, phosphodiester groups in nucleic acids/collagen
1090	Symmetric phosphate stretching vibrations
1240	RNA, Amide III, collagen
1313	Lipid/protein
1330	Collagen, nucleic acids & phospholipids
1450	CH$_2$ bending mode of proteins & lipids, methylene deformation
1557	Tryptophan, tyrosine
1605	Cytocine, phenylalanine, tyrosine, C=C stretch
1667	Protein, C=C stretch, amide I

Table 1. Raman peak assignment (Gelder, 2007, Movasaghi, 2007).

3.1 Statistical analysis of the PIN, BE, and cancer data

The first three eigenvectors or the principal components (PCs) are plotted against each other in Figure 3. The left panel is the plot of PC2 vs. PC1 and the right panel represents PC3 vs. PC1. These three PCs contain 76% of the variance in the data showing different trends for each pathological state. Although some of the data seem to be overlapping with each other, the different trends are still very clear in the data. The largest variance in the data is captured by the PC1 which is shown by the spread of the BE, PIN and cancer along the PC1 axis. PC3 shows distinct trend present in the spectral data of PIN.

The average spectra of BE, PIN, and cancer showed distinct variations in the intensities of certain peaks while the spectral features of individual spectrum of each category are expected to spread about its average value and must also be different from other categories. As tissue changes from BE to PIN and then to cancer, the spectral variances in the data must exhibit some distinct classes if each of these categories is pathologically different. The classification results are shown in Figure 4 where we clearly see three distinct classes with their centroids (marked with black squares) far away from each other. It is interesting to note that PIN class is very distinct class from other classes and does not have much overlap

with others. There are only three pathological states (Klecka, 1980), which means there are two discriminant functions (DFs). So the DF1 shows the maximum variance in the Raman data, and the DF2 contains the rest of the variances.
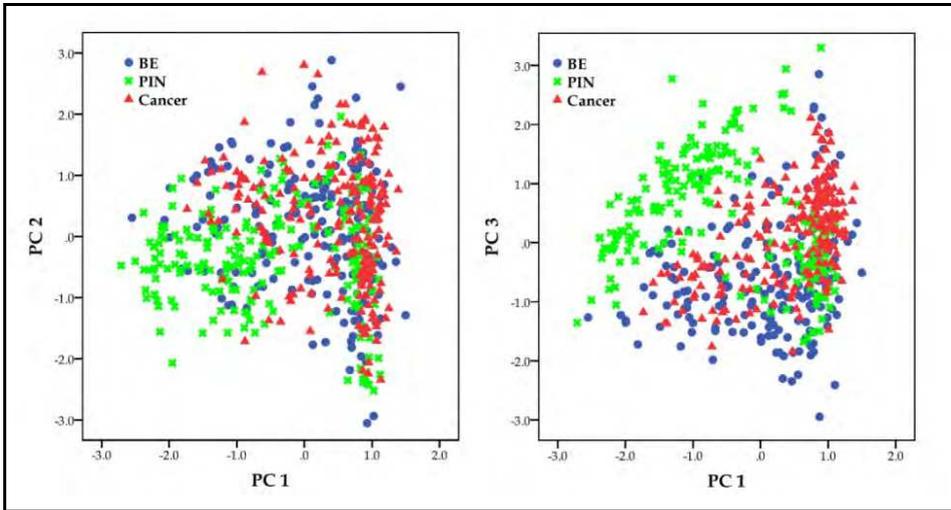

Fig. 3. PCA results of BE, PIN, and cancer. PC2 vs PC1 is on the left panel and the PC3 vs. PC1 is on to the right.
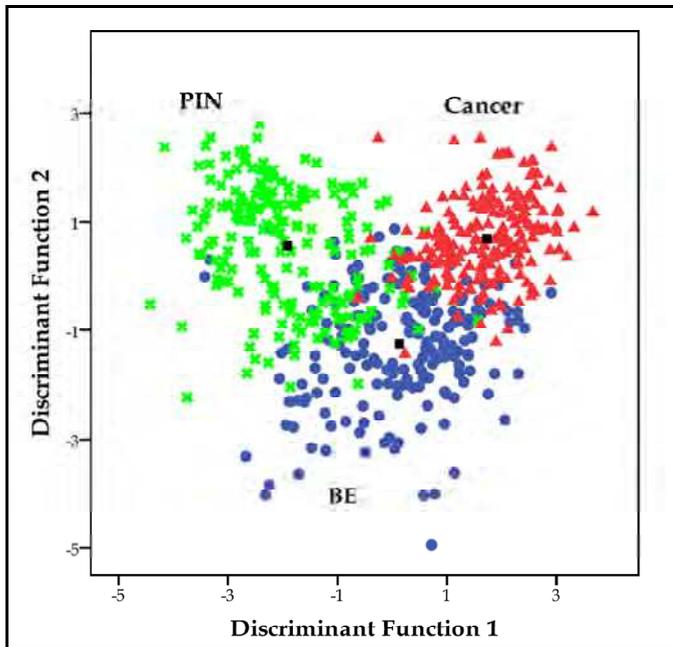

Fig. 4. DF plot of BE, PIN, and cancer.

			Predicted Group Membership			
		Group	BE	PIN	Cancer	Total
Cross-validated	Count	BE	158	20	29	207
		PIN	33	165	4	202
		Cancer	16	2	190	208
	%	BE	**76.3**	9.7	14.0	100.0
		PIN	16.3	**81.7**	2.0	100.0
		Cancer	7.7	1.0	**91.3**	100.0

Table 2. Classification results of BE, PIN, and cancer. Centre the values of "BE", "PIN" and "Cancer"

The group prediction of the Raman spectroscopy data using DFA is compared with that of pathological diagnosis: the "gold standard" for diagnosing cancer. To test the validity of our predicted classifications, we have performed leave-one-out cross-validation where the group classification for each spectrum with one of the known pathological states is determined while using the remaining data as a training set. The results of cross-validation classification results are shown in Table 2. We see that the PIN is predicted with 82% accuracy while the prediction accuracies for BE and cancer are 76% and 91 %, respectively.

3.2 Comparison of Raman spectra of stroma in BE, PIN, and cancer

It is interesting to study the stroma surrounding each of the pathological states as it could provide useful information about the onset of cancer. The nature of stroma observed was found to depend on its environment (Bowsher & Carter, 2006). Figure 5 shows the average Raman spectra of stroma surrounding BE, PIN, and cancer. The stroma surrounding cancer shows a significant enhancement in the intensity of Raman bands at 726, 758, 931, 1240, 1313, and 1330 cm^{-1} compared to stroma surrounding PIN and BE whereas bands at 1081, 1450 and 1667 cm^{-1} show a slight reduction in intensity. The Raman spectra of stromal regions in cancer and BE seem to show similarity in their biochemicals compared to that of the stroma of PIN. When comparing spectral features of the luminal cells of PIN with surrounding stroma, the Raman bands associated with DNA/RNA (726, 780, 829, and 1330 cm^{-1}) are suppressed and the bands arising from amino acids/protein/collagen (853, 931, 960, and 1240 cm^{-1}) are significantly enhanced. This can also be observed in the stroma of BE, and cancer.

The chemometric analysis was also performed on the stromal data. The PC plots of stromal investigation are shown in Figure 6. Here, the analysis generated 15 principal scores containing 98% of the variance in the Raman data. The plot is based on the first three PCs which consist of 86% of the Raman spectral information. Here, we see clear trends for stroma associated with each epithelial category: BE, PIN, and cancer.
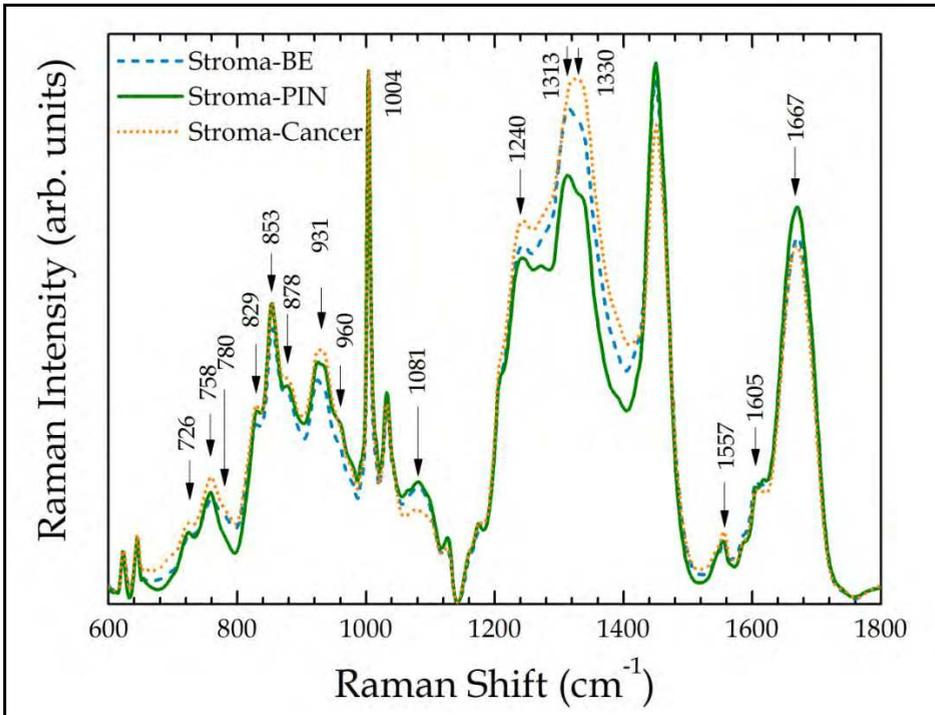
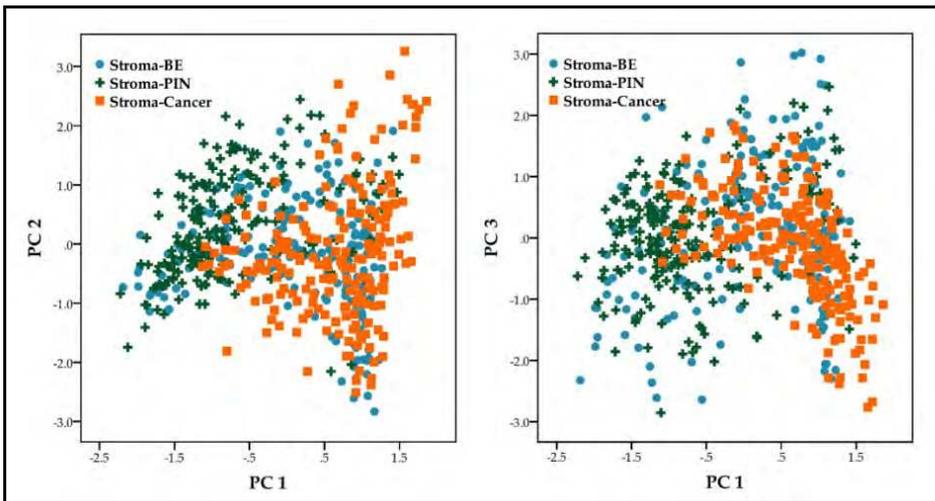Fig. 5. Average Raman spectra of stroma surrounding BE, PIN, and cancer.

Fig. 6. PCA analysis of the Raman data of stroma.

Apparently, the stroma surrounding BE, PIN, and cancer are quite distinct as shown in the DF plot together with the overlapping average Raman spectra of stroma in BE, stroma in PIN, and stroma in cancer (see Figures 6 and 7).   Here, the DFA is performed with 15 eigenvectors which contained 98% of the variance in the stromal data.   Table 3 shows predicted group membership using leave-one out classification method for stromal investigation, we find that the stroma surrounding PIN is 83.6% correctly identified.   The stroma in BE and cancer is classified with 81.6% and 87.1% accuracy, respectively.

It seen that when comparing stroma surrounding PIN with that of cancer, the intensities of Raman bands at 853, 931, 1240, and 1330 cm^{-1} have increased whereas the Raman bands at 1081 cm^{-1} and 1450 cm^{-1} have decreased.   Thus, Raman spectroscopy can be used to distinguish easily the stroma associated with BE, PIN, and cancer accuracy.   It is interesting to note when spectral data of all the pathologies are combined and analyzed statistically to find their distinct classes, we see a clear separation of stroma from BE, PIN and cancer.   In addition stroma of BE, PIN, and cancer are also well separated (see Figure 8).

It should be noted that DFA constructs one less number of discriminant functions for the user-defined categories. Thus, this analysis created 5 discriminat functions due to 6 categories, and figure 8 shows only the first two discriminant functions which carry 89% of the variance in the Raman spectra.   Thus, the overlapping of data in this 2-D plot may not be the same for the other dimensions.   This study shows that the Raman spectroscopy can be used to distinguish the luminal cells in their normal, BE and PIN states. Further, the stroma surrounding these regions can also be distinguishes as they exhibit distinct characteristic spectral features of their own.
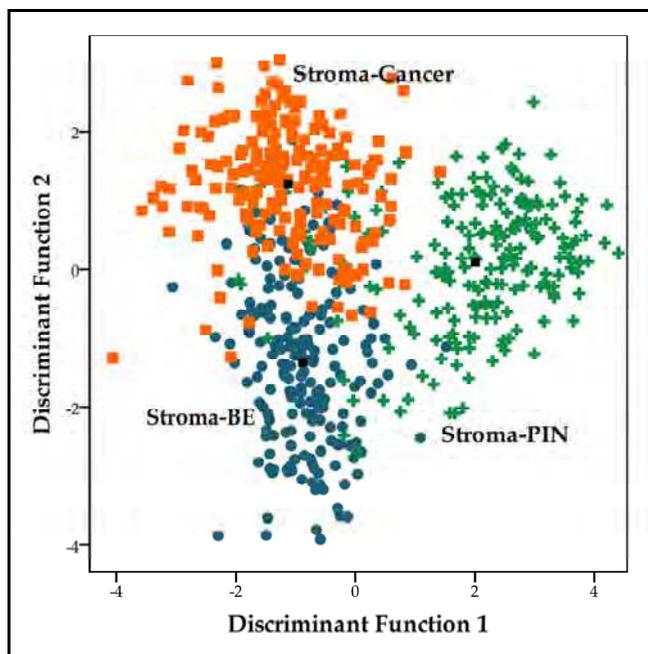

Fig. 7. DF plot of stroma surrounding BE, PIN, and cancer.

			Predicted Group Membership			
		Group	Stroma-BE	Stroma-PIN	Stroma-Cancer	Total
Cross-validated	Count	Stroma-BE	164	3	34	201
		Stroma-PIN	14	168	19	201
		Stroma-Cancer	18	8	175	201
	%	Stroma-BE	**81.6**	1.5	16.9	100.0
		Stroma-PIN	7.0	**83.6**	9.5	100.0
		Stroma-Cancer	9.0	4.0	**87.1**	100.0

Table 3. Classification results of stroma in BE, PIN, and cancer.
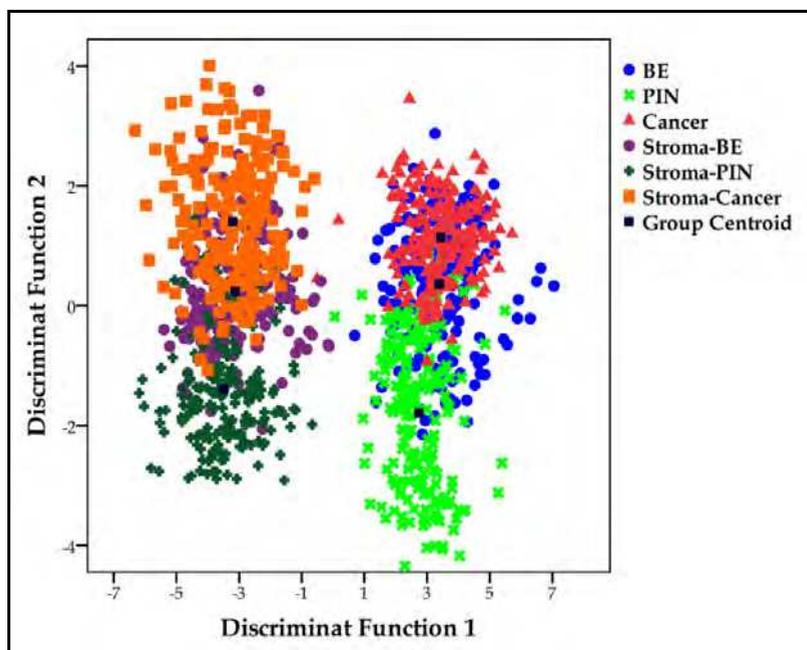
Fig. 8. DF plot of all the categories: BE, PIN, and cancer, and their surrounding stroma.
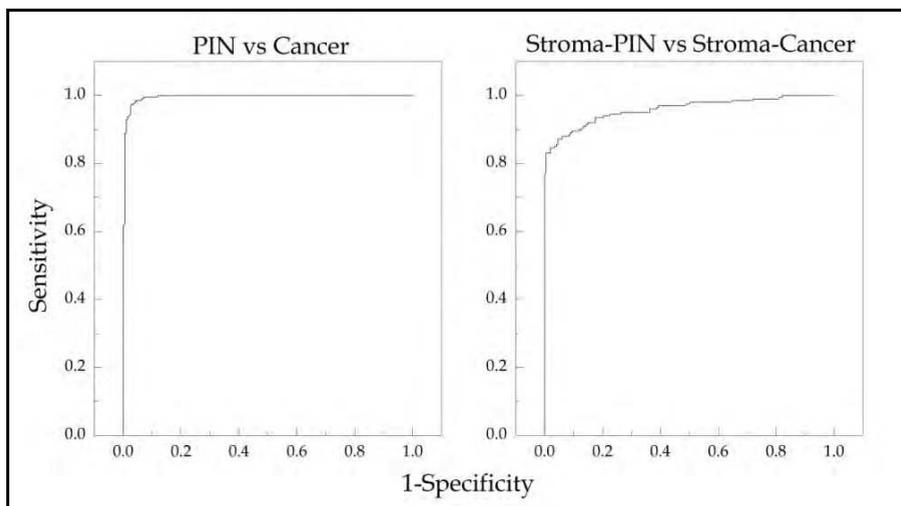
Fig. 9. ROC curves for PIN vs cancer and stromal PIN vs stromal cancer.

We also constructed Receiver Operating Characteristic (ROC) curves (Mason & Graham, 2002) for both the analyses, PIN compared to cancer and comparison between stroma around PIN and stroma associated with cancer. In an ROC graph, the sensitivity and 1-specificity are plotted against each other. Sensitivity is the ratio of true positives (cancer measurements which are correctly identified as cancer) over the total PIN data and the specificity is the ratio of true negatives (PIN measurements which are correctly identified as PIN) over the total PIN data. The sensitivity and specificity for luminal cell investigation of PIN and cancer are 98% and 99%. For the stromal investigation, the sensitivity and specificity are about 90% and 94%, respectively. The area under the curves (AUC) infers the validity of the test. An AUC = 1, indicates a perfect test whereas AUC = 0.5 implies a null result. As shown in Figure 9, both the AUC's are more than 0.96 indicating a very good test for PIN and stroma investigations.

4. Conclusions and future work

In this study, we have investigated using Raman spectroscopy, luminal cells from the tissues which are purely either BE, PIN or cancerous. We particularly focused on PIN and compared its spectral features with BE and cancer. Significant and noticeable changes in the Raman spectra of BE, PIN, and cancerous tissues are observed. As luminal cells become cancerous, the intensities of the most Raman bands in the 700-1000 cm^{-1} increase and the intensity changes can be interpreted in terms of changes in the biochemical composition of the tissues. In particular, the intensity of the 780 cm^{-1} (possibly arising from nucleic acids) Raman band increases considerably in the spectrum of cancerous tissue compared to the BE. Additionally, we also studied stromal cells surrounding each pathological state of the tissues, namely, BE, PIN and cancer and, we observed enhancement in protein contents and reduction in DNA contents when compared to the luminal cells. Chemometric analysis of the data shows that the spectral variations in the data are quite pronounced and can easily be classified with very high accuracies into distinct pathological groups. The sensitivity and

specificity of luminal cells of PIN and cancer are about 98% for each and for the stroma associated with these pathologies, both the sensitivity and specificity are more than 90%. Current study suggests further investigation of different pathology grades (low and high grade) of PIN, including basal cells, are needed and to expand the Raman spectral database for better prediction capability. Since some of the PIN structures may not lead to carcinoma, by spectroscopic investigation one can explore the Raman signatures of a PIN structure which can lead to cancer.

5. Acknowledgement

6. References

Allsbrook, W. C. , Mangold, K. A., Johnson, M. H., Lane, R. B., Lane, C. G. & Epstein, J. I. (2001). Interobserver reproducibility of Gleason grading of prostatic carcinoma: General Pathologists. *Human Pathology*, Vol. 32, No. 1, (January 2001), pp. (81-88)

Andriole, G. L., Bullock, T. L., Belani, J. S., Traxel, E., Yan, Y., Bostwick, D. G. & Humphrey, P. A. (2007). Is there a better way to biopsy the prostate? Prospects for a novel Transrectal systematic biopsy approach. *Urology*, Vol. 70, No. 6, Supp 6A, (December 2007), pp. (22-26).

Bostwick, D. G. & Qian, J. (2004). High-grade prostatic intraepithelial neoplasia. *Modern Pathology*, Vol. 17, (January 2004), pp. (360–379).

Bowsher, W & Carter, A. (2006). *Challenges in prostate cancer* (Second edition), Blackwell Publishing, ISBN 978-4051-0752-5, Massachusetts, USA.

Cao, A., Pandya, A. K., Serhatkulu, G. K., Weber, R. E., Dai, H., Thakur, J. S., Naik, V. M., Naik, R., Auner, G. W. & Rabah, R. J. (2007). A robust method for automated background subtraction of tissue fluorescence. *J Raman Spectrosc.*, Vol. 38, (May 2007), pp. (1199–1205)

Carroll, P., Alnerstein , P. C., Greene, K., Babalan, R. J. , Carter, H. B., Gann, P. H., Han, M., Kuban, D. A., Sartor, A. O., Stanford, J. L. & Zletman, A. (2009). In: *Prostate-Specific Antigen Best Practice Statement,* http://www.auanet.org/content/guidelines-and-quality-care/clinical-guidelines/main-reports/psa09.pdf.

Crow, P., Molckovsky, A., Stone, N., Uff, J., Wilson, B. & Wongkeesong, L.-M. (2005). Assesment of fiberoptic near-infrared Raman spectroscopy for diagnosis of bladder and prostate cancer. *Urology*, Vol. 65, (June 2005), pp. (1126-1130)

Crow, P., Stone, N., Kendall, C. A., Uff, J. S., Farmer, J. A. M., Barr, H. & Wright, M. P. J. (2003). The use of Raman spectroscopy to identify and grade prostatic adenocarcinoma in vitro. British J of Cancer, Vol. 89, pp. (106-108)

Devpura, S., Thakur, J. S., Sarkar, F. H., Sakr, W. A., Naik, V. M. & Naik, R. (2010). Detection of benign epithelia, prostatic neoplasia, and cancer regions in radical prostatectomy tissues using Raman spectroscopy. *Vibrational Spectrosc.,* Vol. 53, (July 2010), pp. (227-232)

Devpura, S., Thakur, J. S., Sethi, S, Naik, V. M. & Naik, R. (2011). Diagnosis of head and neck squamous cell carcinoma using Raman spectroscopy: tongue tissues. *J Raman Spectrosc.* (DOI: 10.1002/jrs.3070)

Fleshner, N. E., Kapusta, L., Donnelly, B., Tanguay, S., Chin, J., Hersey, K., Farley, A., Jansz, K., Siemens, R., Trpkov, K., Lacombe, L., Gleave, M., Tu D. & Parulekar, W. R. (2011). Progression From High-Grade Prostatic Intraepithelial Neoplasia to Cancer: A Randomized Trial of Combination. *J Clin. Oncol.*, Vol. 29, (June 2011), pp. (2386-2390)

Gelder, J. D., Gussem, K. D., Vandenabeele, P & Moens, L. (2007). Reference database of Raman spectra of biological molecules. *J Raman Spectrosc*. Vol. 38, (September 2007), pp. (1133-1147).

Hayward, S. W., Wang, Y., Cao, M., Hom, Y. K. & Zhang, B. (2001). Malignant transformation in a nontumorigenic human prostatic epithelial cell line. *Cancer Res.*, Vol. 61, (November 2001), pp. (8135–8142).

Hricak, H., Scardino, P. T. & Reznek, R. H. (2009). *Prostate Cancer*, Cambridge University Press, ISBN 978-0-521-88704-5, New York, USA.

Humphrey, P. A. (2004). Gleason grading and prognostic factors in carcinoma of the prostate. *Modern Pathology*, Vol. 17, (March 2004), pp. (292–306), doi:10.1038/ modpathol.3800054.

Jemal, A., Siegel, R., Bray, F., Center, M. M., Ferlay, J., Ward, E. & Forman, D. (2011). Global Cancer Statistics. *Cancer J Clin.* Vol. 5961, (March/April 2011), pp. (225-249), doi:0.3322/caac.20107 doi: 10.3322/caac.20006.

Jolliffe, I. T. (2002). *Principal Components Analysis* (Second edition), Springer-Verlag, New York, USA.

Kandaswami, C., Lee, L. T., Lee, P. P, Hwang, J. J., Ke, F. C., Huang, Y. T. & Lee, M. T. (2005). The antitumor activities of flavonoids. *In Vivo*, Vol. 19, (September-October 2005), pp. (895-909).

Keller, M. D., Kanter, E. M. & Mahadevan-Jansen A. (2006). Raman spectroscopy for cancer diagnosis. Spectroscopy, Vol. 21, No. 11, (November 2006), pp. (33-41)

Klecka, W. R. (1980). *Discriminant Analysis, Series: Quantitative applications in the social sciences*, Sage Publications Inc., Newbury Park.

Laserna, J. J. (1996). *Modern Techniques in Raman spectroscopy*, John Wiley& Sons, New York, USA.

Mason, S. J.& Graham, N. E. (2002). Areas beneath the relative operating characteristics (ROC) and relative operating levels (ROL) curves: Statistical significance and interpretation. *Q. J. R. Meteor. Soc*. Vol. 128, pp. (2145-2166).

Movasaghi, Z., Rehman, S. & Rehman, I. U. (2007). Raman spectroscopy of biological tissues. *Applied. Spectroscopy Reviews,* Vol. 42, (September 2007), pp. (493-541), doi: 10.1080/05704920701551530.

Niu, Y. -N. & Zia, S. -J. (2009). Stroma–epithelium crosstalk in prostate cancer. *Asian Journal of Andrology*, Vol. 11, (December 2008), pp. (28–35).

Oesterling, J. E. (1991). Prostate specific antigen: a critical assessment of the most useful tumor marker for adenocarcinoma of the prostate. *J Urol,* Vol. 145, No. 5, (May 1991), pp. (907-923).

Ó Faoláin, E., Hunter, M. B., Byrne, J. M., Kelehan, P., Lambkin, H. A., Byrne, H. J. & Lyng, F.M. (2005). Raman Spectroscopic Evaluation of Efficacy of Current Paraffin Wax

Section Dewaxing Agents *J Histochem Cytochem* Vol. 53(1), (March 2005), pp. (121-129).

Olumi, A. F., Grossfeld, G. D., Hayward, S. W., Carroll, P. R., Tlsty, T. D. & Cunha, G. R. (1999). Carcinoma-associated fibroblasts direct tumor progression of initiated human prostatic epithelium. *Cancer Res*, Vol. 59, (October 1999) pp. (5002–5011).

Partin A. W., Kattan, M. W., Subong, E. N., Walsh, P. C., Wojno, K. J., Oesterling, L. E., Scardino, P. T., & Pearson, J. D. (1997). Combination of prostate-specific antigen, clinical stage, and Gleason score to predict pathological state of localized prostate cancer. A multi-institutional update. *J. Am. Med. Assoc.,* Vol. 277, (May 1997), pp. (1445–1451).

Quinn, D. I., Henshall, S. M., Brenner, P. C., Kooner, R., Golovsky, D., O'Neill, G. F., Turner, J. J., Delprado, W., Grygiel, J. J., Sutherland, R. L. & Stricker, P. D. (2003). Prognostic significance of preoperative factors in localized prostate carcinoma treated with radical prostectomy. *Cancer*, Vol. 97, No. 8, (April 2003), p.p. (1884-1893).

Raman, C. V. (1928). A new type of secondary radiation. *Nature*, Vol. 121, No. 3048, (March 1928), pp. (501-502).

Saha, A. & Yakovlev, V. V. (2009). Towards a rational drug design: Raman micro-spectroscopy analysis of prostate cancer cells treated with an aqueous extract of Nerium Oleander. *J. Raman Spectrosc.,* Vol. 40, (December 2008), pp. (1459–1460).

Shroder, F. H., Hugosson, J. & Roobol, M. J. (2009). Screening and prostate-cancer mortality in a randomized European study. *New Eng J Med*, Vol. 360, (March 2009), pp. (1320-1328).

Smith, Z. J. & Berger, A. J. (2009). Construction of an integrated Raman- and angular-scattering microscope. *Review of Scientific Instruments*, Vol. 80, No. 044302, (April 2009), pp. (1-8).

Stone, N., Kendall, C., Smith, J., Crow, P. & Barr, H. (2003). Raman spectroscopy for identification of epithelial cancers. *Faraday Discuss*, Vol. 126, (September 2003), pp. (141–157).
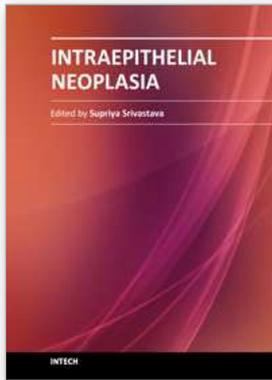
Intraepithelial Neoplasia

Edited by Dr. Supriya Srivastava

The book "Intraepithelial neoplasia" is till date the most comprehensive book dedicated entirely to preinvasive lesions of the human body. Created and published with an aim of helping clinicians to not only diagnose but also understand the etiopathogenesis of the precursor lesions, the book also attempts to identify its molecular and genetic mechanisms. All of the chapters contain a considerable amount of new information, with an updated bibliographical list as well as the latest WHO classification of intraepithelial lesions that has been included wherever needed. The text has been updated according to the latest technical advances.This book can be described as concise, informative, logical and useful at all levels discussing thoroughly the invaluable role of molecular diagnostics and genetic mechanisms of the intraepithelial lesions. To make the materials easily digestive, the book is illustrated with colorful images.

How to reference

In order to correctly reference this scholarly work, feel free to copy and paste the following:

INTECH
open science | open minds